

Comparative proteomic analysis of outer membrane protein 43 (*omp43*)-deficient *Bartonella henselae*

Jun-Gu Kang, Hee-Woo Lee, Sungjin Ko, Joon-Seok Chae*

Laboratory of Veterinary Internal Medicine, Research Institute and BK21 Program for Veterinary Science and College of Veterinary Medicine, Seoul National University, Seoul 08826, Korea

Outer membrane proteins (OMPs) of Gram-negative bacteria constitute the first line of defense protecting cells against environmental stresses including chemical, biophysical, and biological attacks. Although the 43-kDa OMP (OMP43) is major porin protein among *Bartonella henselae*-derived OMPs, its function remains unreported. In this study, OMP43-deficient mutant *B. henselae* ($\Delta omp43$) was generated to investigate OMP43 function. Interestingly, $\Delta omp43$ exhibited weaker proliferative ability than that of wild-type (WT) *B. henselae*. To study the differences in proteomic expression between WT and $\Delta omp43$, two-dimensional gel electrophoresis-based proteomic analysis was performed. Based on Clusters of Orthologous Groups functional assignments, 12 proteins were associated with metabolism, 7 proteins associated with information storage and processing, and 3 proteins associated with cellular processing and signaling. By semi-quantitative reverse transcriptase polymerase chain reaction, increases in *tldD*, *efp*, *ntrX*, *pdhA*, *purB*, and ATPA mRNA expression and decreases in *Rho* and *yfeA* mRNA expression were confirmed in $\Delta omp43$. In conclusion, this is the first report showing that a loss of OMP43 expression in *B. henselae* leads to retarded proliferation. Furthermore, our proteomic data provide useful information for the further investigation of mechanisms related to the growth of *B. henselae*.

Keywords: *Bartonella*, *omp43*, outer membrane protein, proliferation, proteomics

Introduction

Bartonella henselae is a widely distributed, Gram-negative, slow-growing, fastidious, facultative intracellular bacterium causing various diseases including bacillary angiomatosis, bacillary peliosis, and cat scratch disease (CSD) [2]. The transmission of *B. henselae* to humans is associated with exposure to *B. henselae*-infected cats and fleas [22]. CSD is usually a self-limiting inflammation of the lymph nodes near the scratch site. In immunocompromized patients, *B. henselae* causes tumorous proliferation of endothelial cells in internal organs, as well as a recurrent infection that can persist for a prolonged period [22]. Exposure of primary human umbilical vein cells (HUVEC) to *B. henselae* has been shown to result in bacterial aggregation on the cell surface, and subsequent engulfment and internalization of the bacterial aggregate by the formation of invasomes [13]. One of the most commonly identified pathogenic factors of *B. henselae* is the *Bartonella* adhesion A (BadA) protein located in the outer membrane of the bacterium. BadA mediates the mechanism underlying the

binding of *B. henselae* to extracellular matrix proteins and endothelial cells, and it activates hypoxia-inducible factor-1. Moreover, the BadA neck is a major functional domain related to host adhesion, auto-agglutination, and angiogenic reprogramming [20]. On the other hand, *B. henselae* outer membrane proteins (OMPs), as well as *B. henselae* itself, can induce adhesion molecule expression in endothelial cells [15]. In the sarcosyl-insoluble fraction of *B. henselae* lysates, nine proteins were detected, five of which (28, 32, 43, 52, and 58 kDa) were attached to HUVECs [6]. Moreover, Dehio *et al.* [13] have suggested that the 43-kDa OMP (OMP43) is the major adhesin among *B. henselae*-derived OMPs that interacts with HUVEC.

The outer membranes of Gram-negative bacteria determine the molecules to be taken in or excreted by the cells. Moreover, in many bacteria, the outer membrane is the predominant layer that interacts with antibodies and other proteins. Porins, which were discovered in 1976, are the major proteins of the outer membrane and are found in every Gram-negative species [26]. Nonspecific diffusion of hydrophilic solutes across the outer

Received 20 Mar. 2017, Revised 9 May 2017, Accepted 8 Jun. 2017

*Corresponding author: Tel: +82-2-880-1279; Fax: +82-2-873-1213; E-mail: jschae@snu.ac.kr

Journal of Veterinary Science · © 2018 The Korean Society of Veterinary Science. All Rights Reserved.

This is an Open Access article distributed under the terms of the Creative Commons Attribution Non-Commercial License (<http://creativecommons.org/licenses/by-nc/4.0>) which permits unrestricted non-commercial use, distribution, and reproduction in any medium, provided the original work is properly cited.

pISSN 1229-845X

eISSN 1976-555X

membrane usually occurs through porin channels with distinctive diameters. Consequently, porins are the major uptake/excretory route for nutrients, toxins, antibiotics, hydrolytic enzymes, *etc.* [28]. On the other hand, some researchers were reported that the OMP43 sequence of *B. henselae* showed 38% identity and 53% similarity to the Omp2b porin of *Brucella* species [7]. In addition, *B. henselae* OMP43 showed homology to the proteins of *Rhizobium leguminosarum* that may possess pore-forming abilities [12].

These data suggest that *B. henselae omp43* could be a porin-coding gene and that the OMP43 protein interacts with other cells and molecules. This study was aimed at characterizing the proteome of $\Delta omp43$ and comparing it to that of the wild-type (WT) strain by applying proteomic methods, which can help elucidate the pathogenesis of *B. henselae*. In addition, we performed semi-quantitative reverse transcriptase polymerase chain reaction (RT-PCR) to confirm the proteomic data.

Materials and Methods

Bacterial strains and growth conditions

B. henselae strain Houston-1 (ATCC 49882) was cultured on Columbia blood agar plates containing 5% defibrinated sheep

blood (BAP-agar plates) in a humidified atmosphere at 37°C and 5% CO₂. *Escherichia coli* was grown in Luria-Bertani (LB) broth at 37°C.

Construction of p $\Delta omp43$

Primers, plasmids, and bacterial strains used in this study are listed in Table 1 [7,31]. DNA extraction was performed according to standard protocols. Chromosomal DNA was extracted from *B. henselae* (Houston-1) by using DNeasy Blood & Tissue Kits (Qiagen, Germany) according to the manufacturer's instructions.

For construction of the *omp43* plasmid (*pomp43*), the *omp43* gene was amplified by using BamH-*omp43* and *omp43*-Hind primers. The amplicon was cloned with pGEM-T Easy Vectors (Promega, USA), followed by transformation into *E. coli* DH5 α . Purification of plasmid DNA was performed by using the Wizard Plus SV Minipreps DNA Purification System (Promega) according to the manufacturer's instructions. The pBluescript II KS plasmid and T vector containing *omp43* sequences were digested with BamH I and Hind III. The insert (containing the *omp43* gene) was ligated into the pBluescript II KS vector and transferred into *E. coli* DH5 α .

A kanamycin resistance gene (Km^r) was amplified from pET-28 α by using Sph I-km-F and Sph I-km-R primers, cloned

Table 1. Bacterial strains, plasmids, and primers used in this study

	Characteristic or sequence	Reference or source
Strains		
<i>Bartonella henselae</i>		
Wild-type	<i>B. henselae</i> Houston-1, ATCC 49882	[31]
$\Delta omp43$	<i>B. henselae omp43</i> deficient mutant, Km ^r	This study
<i>Escherichia coli</i>		
DH 5 α	Host strain used for cloning	Invitrogen
Top 10	Host strain used for cloning	Invitrogen
BL21 (DE3)	Host strain used for protein expression	Stratagene
Plasmids		
pGEM-T easy	Vector for cloning, Ap ^r	Promega
pET-28a	Vector for protein expression, Km ^r	Novagen
pBAD/His	Vector for protein expression, Ap ^r	Invitrogen
pBluescript II KS	Vector for homologous recombination, Ap ^r	Stratagene
<i>pomp43</i>	pBluescript II KS containing a 1.2 kb of <i>B. henselae omp43</i> fragment, Ap ^r	This study
p $\Delta omp43$	<i>pomp43</i> containing a kanamycin cassette in the middle site of <i>omp43</i> gene sequence, Ap ^r , Km ^r	This study
Primers		
Bgl- <i>omp43</i>	ctgagatctgcttcaaacgtttattgcag	[7]
<i>omp43</i> -EcoR	cggaattcttaaaatgaacgttgaagcg	[7]
BamH- <i>omp43</i>	gagaggatccaaatgaatgtaag	This study
<i>omp43</i> -Hind	gagaaagcttttaaaatgaacgttgaagcg	This study
Sph1-km-F	gagagcatgcaaatgagccatattca	This study
Sph1-km-R	gagagcatgcttagaaaaactcatcgag	This study

with pGEM-T Easy Vector as previous described. After purifying, the T vector containing Km^r together with *pomp43* were digested with Sph I and then the cut Km^r was ligated with *pomp43* (middle region of *omp43* gene sequences). As a result, the p Δ *omp43* plasmid was acquired. Additionally, the p Δ *omp43* sequence was confirmed by dideoxy termination with an automatic sequencer (ABI 3730xl capillary DNA sequencer, Applied Biosystems, USA).

Expression of OMP43

The OMP43 of *B. henselae* was prepared as described previously [7]. Briefly, *omp43* without the signal peptide was amplified from *B. henselae* (Houston-1) by using Bgl-*omp43* and *omp43*-EcoR primers. The pBAD/His B plasmid and the *omp43* PCR product were digested using restriction enzymes (Bgl II and EcoR I). The digested *omp43* amplicon was cloned with the digested pBAD/His B vector, followed by transformation into *E. coli* TOP10. OMP43 was expressed by induction with 0.02% arabinose for 6 h at 37°C in LB containing 50 mg/mL ampicillin. The denatured samples were separated by 12% sodium dodecyl sulfate-polyacrylamide gel electrophoresis (SDS-PAGE) and transferred to a nitrocellulose membrane. OMP43 protein was detected by western blotting using the anti-Xpress antibody (Invitrogen, USA) and anti-mouse IgG secondary antibody (Cell Signaling, USA) (data not shown).

Purifying and polyclonal antibody production of OMP43

Purified recombinant OMP43 was acquired by Ni²⁺ affinity chromatography (via request to Bio Basic, USA). Briefly, induced bacteria were harvested by centrifugation and then sonicated on ice in lysis buffer. The OMP43 fusion protein inclusion bodies were diluted into refolding buffer, 1 mM GSSG (oxidized glutathione), and stirred at 4°C for 24 h. The dissolved OMP43 fusion protein solution underwent dialysis against a buffer solution. The refolded protein was harvested by centrifugation for 20 min at 30,000 × g and then digested with an enterokinase at 4°C for 24 h. Subsequently, the digested *omp43* protein was purified by Ni²⁺ affinity chromatography.

For production of the polyclonal antibody against OMP43, an OMP43-specific rat antiserum was raised by immunization with purified OMP43 for 9 weeks and purified by affinity chromatography.

Electroporation of *B. henselae*

Five-day-old *B. henselae* were harvested from 2 BAP-agar plates with a sterile cotton swab into ice-cold distilled water (DW) containing 10% glycerol. Competent cells were prepared by washing three times with ice-cold DW containing 10% glycerol. The pellet was resuspended in 100 µL of ice cold DW containing 10% glycerol in a cooled electroporation 0.1-cm-gap cuvette (BioRad, USA). Subsequently, 10 µL of the p Δ *omp43* plasmid solution (2 µg/µL) was added into the cuvette and

gently mixed before being allowed to stabilize on ice for 15 min. Electroporation was conducted with a field strength of 1.2 kV/cm and a constant capacitance of 25 µF at 200 Ω. Electroporated cells were immediately transferred into 1 mL super broth (SB) broth at room temperature. Subsequently, cells were incubated for 4 h at 37°C in 5% CO₂ and then seeded on BAP-agar plates containing kanamycin.

Growth curve

For the comparison of growth abilities of WT and Δ *omp43*, counted bacteria (100,000 colony-forming unit [CFU]) were seeded on BAP-agar plates and incubated in a humidified atmosphere at 37°C and 5% CO₂. After harvesting from BAP-agar plates with a sterile cotton swab, the bacteria were resuspended in phosphate buffered saline (PBS). Optical density (OD) was estimated on 600 nm.

Two-dimensional proteomics

Whole cell protein extractions: For whole cell protein extraction, cells were harvested from BAP-agar plates and resuspended in iced PBS. Bacteria were washed three times with iced PBS, centrifuged, and resuspended in lysis buffer. Subsequently, cells were broken by sonication using a Branson sonifier (Thermo Fisher Scientific, USA) until the solution turned an opaque yellow color. By centrifugation at 30,000 × g at 4°C for 40 min, the debris was pelleted. The supernatant contained solubilized whole cell lysate, which was quantified using the RC/DC Protein Assay kit (BioRad) according to the manufacturer's protocol.

Two-dimensional SDS-PAGE: Whole cell proteins were separated in the first dimension by using immobilized pH 3 to 10 nonlinear gradient strips (Amersham Biosciences, UK). Isoelectric focusing of the protein-containing samples was performed in a protein IEF cell (BioRad). Afterward, second-dimension analysis was performed on 9% to 16% linear gradient polyacrylamide gels, and protein fixation was performed. They were scanned in a Biorad GS710 densitometer (BioRad) and the results converted into electronic files and were analyzed by using the Image Master Platinum 5.0 image analysis program (Amersham Biosciences). Analysis was conducted to identify spots with a minimum 2-fold increased or decreased difference between *B. henselae* Houston-1 (ATCC49882) and kanamycin-resistant *omp43* deficient *B. henselae* (Δ *omp43*).

Matrix-assisted laser desorption ionization-time of flight-mass spectrometry (MALDI-TOF-MS):

Protein processing

Selected spots were excised from stained two-dimensional (2D) gels by using an Ettan spot picker (GE Healthcare, UK) and then transferred into 96-well plates. Tryptic digestion with subsequent spotting on a MALDI-target was carried out automatically with the Ettan Spot Handling Workstation (GE

Table 2. Primers for reverse transcriptase polymerase chain reaction in this study

Gene	Forward primer	Reverse primer	Expected bp
<i>tldD</i>	CAAAGCCAGAAAAAGCAG	TGGGAATCTGTGCGTGATA	328
<i>Rho</i>	CTTCTTCTGGCCTTTCATCG	CCTGCGCAAATTCATCTTT	400
<i>efp</i>	AGGTGGCGCATTTAATCAAG	ATTTCACGACGCACATAAA	463
<i>ntxX</i>	AAATGCTGCAACGATTACCC	ACAAAATGGCGGACAAGTTC	381
<i>pdhA</i>	AGGGGACAGTTTACGAAAAGT	TCAATCGGATCCTGTTCTC	355
<i>purB</i>	CTTTGCAACGCTTGGTGTTA	AGTCGAGCGAGAGCAAAGTC	315
ATPA	ACGTGGAATAATGCCTGGAG	CTCGCGTTTATGGTTGGAT	302
<i>yfeA</i>	TGTCTCCGACTTCAGCATTG	TCCAACTTGTTTAGCAGGA	375
16S	CGATCCAGCCTAACTGAAGG	TTGTTCCGATTACTGGGCGTA	493

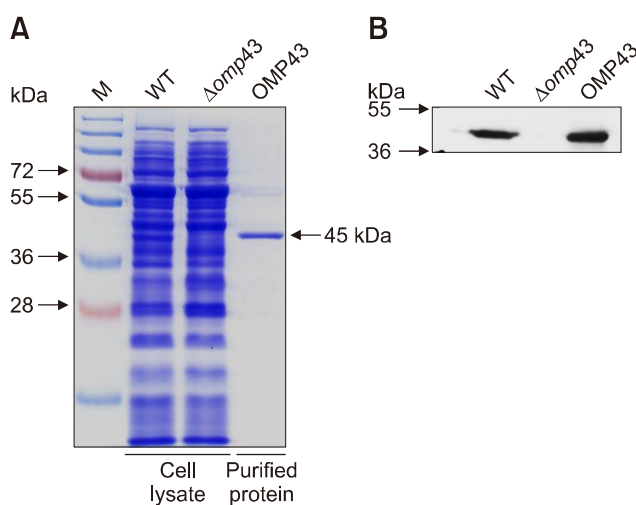


Fig. 1. (A) Coomassie blue stained sodium dodecyl sulfate-polyacrylamide gel electrophoresis analysis of *Bartonella henselae* wild-type strain, *omp43* deficient mutant strain ($\Delta omp43$), and purified outer membrane protein 43 protein (OMP43). M, protein marker; WT, wild-type strain cell lysate. (B) Western blotting analysis of WT and $\Delta omp43$.

Healthcare). After drying at 37°C for 15 min, a trypsin solution was added and incubated at 37°C for 2 h. Subsequently, pieces were covered with 50% CH₃CN (0.1% trifluoroacetic acid [TFA]) and incubated for 30 min. The dried samples were dissolved in 50% CH₃CN (0.5% TFA) and directly spotted on the MALDI-target. The samples were mixed with saturated a cyano-4-hydroxycinnamic acid solution in 70% CH₃CN and allowed to dry on the target before measurement in MALDI-TOF.

Protein measurements

The MALDI-TOF-MS was conducted on 4800 MALDI-TOF/TOF Analyzer (Applied Biosystems) equipped with a 355-nm Nd:YAG laser. The mass spectra were analyzed in the reflectron mode and using the 4700 calibration mixture (Applied Biosystem). The SD of the mass was less than 0.15 Da.

After calibration, peak lists were obtained by using the 'Peak to MASCOT' script of 4700 Explorer Software (Applied Biosystems). For protein identification, the peptide mass lists were matched against databases proposed by the search engine Mascot (Matrix Science, UK). To select candidate antigens, the highest sequence coverages and Mascot scores were used. According to the Clusters of Orthologous Groups (COGs) classification, the identified proteins were functionally categorized (National Center for Biotechnology Information, USA).

Semi-quantitative RT-PCR

The WT and $\Delta omp43$ *B. henselae* were cultured for 6 days and harvested from BAP. The RNA was extracted from them by using the Ribopure-bacteria kit (Ambion, USA) according to the manufacturer's instructions. The cDNA synthesis was carried out with the Primescript 1st strand cDNA synthesis kit (Takara, Japan) according to the manufacturer's instructions. The primers used for RT-PCR are listed in Table 2. The PCR conditions were 30 sec at 94°C, 30 sec at 60°C, and 30 sec at 72°C for 20 cycles (16S gene) or 28 cycles (*tldD*, *efp*, *ntxX*, *pdhA*, and ATPA genes) or 29 cycles (*Rho*, *purB*, and *yfeA* genes). PCR amplicons were analyzed by electrophoresis on 1.5% agarose gels and visualized by ethidium bromide staining. RT-PCR band intensities were measured by performing scanning densitometry with the Kodak 1D image analysis software (Eastman Kodak, USA) and analyzed by normalization to 16S rRNA obtained over the same period. Significance of differences was determined by using a Student's *t*-test, and *p* values less than 0.05 were regarded as statistically significant. The data are presented as means \pm SDs.

Results

omp43-targeted mutagenesis using homologous recombination in *B. henselae*

Western blots of OMP43 in *E. coli* revealed a fusion protein of approximately 45 kDa containing a 3 kDa region resulting

from an N-terminal Xpress tag (data not shown). The OMP43 protein was purified using Ni^{2+} affinity chromatography and the purity was confirmed by using SDS-PAGE (Fig. 1).

Kanamycin-resistant *B. henselae* grew to form visible single colonies 2 weeks after electroporation. Several PCRs using

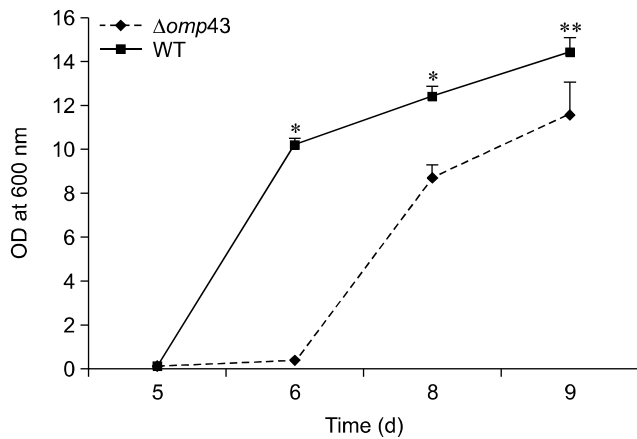


Fig. 2. Growth curve of *Bartonella henselae*. Viable cell counts (reported as OD_{600}) on blood agar plates were determined at 24 h intervals after plating of individual cultures. OD, optical density; WT, wild-type strain; $\Delta omp43$, mutant strain. Data significance was evaluated with a Student's *t*-test; * $p < 0.01$, ** $p = 0.0562$.

primers specific for *omp43*, kanamycin resistance, internal transcribed spacer [34], and 16S rRNA gene sequences were performed to confirm $\Delta omp43$ expression (Table 1). Two kanamycin-resistant *B. henselae* mutants were acquired and the *omp43* gene sequences were confirmed by PCR and sequencing (data not shown).

Additionally, to confirm the expression of OMP43, SDS-PAGE gel staining and western blotting were performed. OMP43 expression in the WT cell lysate was detected by using SDS-PAGE gel staining and western blots, but OMP43 expression in the $\Delta omp43$ lysate could not be detected (Fig. 1). This result showed that there was a complete loss of OMP43 protein expression in $\Delta omp43$.

$\Delta omp43$ grows at slower rate compared to the WT bacterium

On BAP, $\Delta omp43$ grew to form visible single colonies, but at a significantly lower growth rate than that of the WT bacterium. To analyze the difference in the growth rates between $\Delta omp43$ and the WT, we cultured the bacteria on BAP and determined the OD_{600} at 5, 6, 7, 8, and 9 days after seeding. The $\Delta omp43$ showed significantly lower OD than the WT at 6 days (Fig. 2). Additionally, over-grown colonies of $\Delta omp43$ were slightly smaller than those of the WT. This result indicated that *omp43* affected the growth of the *B. henselae* Houston-1 strain.

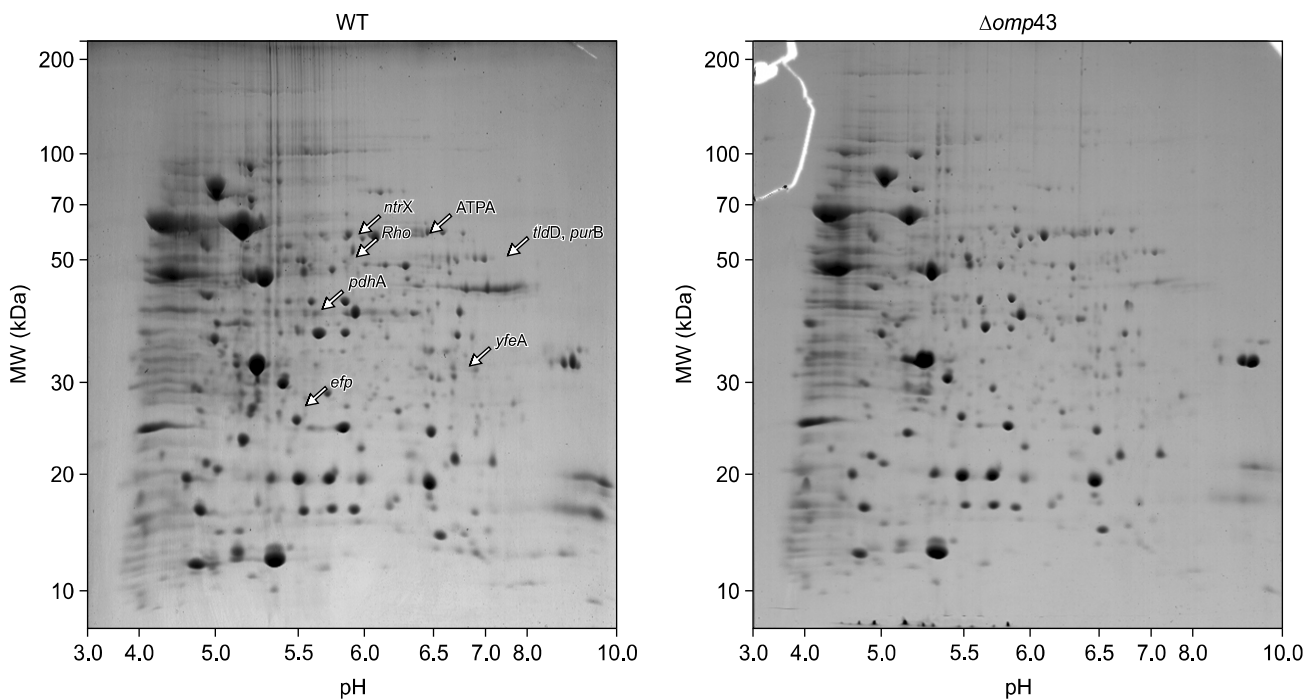


Fig. 3. Two-dimensional sodium dodecyl sulfate-polyacrylamide gel electrophoresis profiles of *Bartonella henselae* wild-type strain (WT, left) and mutant strain ($\Delta omp43$, right). The pH gradient is indicated at the bottom, and molecular mass standard is indicated to the left. The analyzed target proteins by reverse transcriptase polymerase chain reaction are labeled on the panels. Three independent sets of cultures were analyzed, but only one representative set grown on BAP is shown here. MW, molecular weight.

Two-dimensional gel electrophoresis profiles of *B. henselae*

To find new targets associated with *omp43*, total proteins of $\Delta omp43$ and the WT were extracted for 2D gel electrophoresis (2-DE). Representative 2-DE gel images are shown in Fig. 3. In the 2-DE analysis, 422 and 375 protein spots were detected on the 2-DE WT and $\Delta omp43$ gels, respectively. Additionally, 282 paired and 233 non-paired protein spots were identified (Fig. 3). Forty-six protein spots showed a 2-fold change in expression levels. Of the 46 protein spots, 26 showed lower protein expression and 20 showed higher protein expression in $\Delta omp43$ than in the WT.

Analysis of the expressed proteins in $\Delta omp43$

To identify the differentially expressed proteins, 46 of the protein spots selected from the 2-DE gels were excised and subjected to trypsin digestion and subsequent analysis by MALDI-TOF-MS. The 46 protein spots representing 28 different proteins were successfully identified by MALDI-TOF-MS and by MASCOT database searches. Of the identified proteins, 20 showed lower expression and 8 showed higher expression in $\Delta omp43$ than in the WT (Tables 3 and 4). Of these proteins, only the *tldD*-encoded protein displayed both higher and lower expressions, and these two spots were distributed in different parts of immobilized pH gradient (IPG) strips (pH 4.0–5.0 and pH 6.5–7.0, respectively). However, the spot that displayed lower expression and was observed in the part of IPG strip corresponding to pH 6.5–7.0 was more credible than the other spot because of the numerical value of the MASCOT score, the coverage, and the masses matched. This credibility supposition was confirmed by RT-PCR (Fig. 4).

Using categories designated based on the COG database, the differentially expressed proteins could be divided into 4 groups. We found 12 proteins to be associated with metabolism, 7 proteins associated with information storage and processing, 3 proteins associated with cellular processing and signaling, and 6 poorly characterized proteins (Tables 3 and 4). In particular, the number of differentially expressed proteins associated with metabolism indicated that various metabolic processes were affected by the loss of OMP43 expression. Additionally, this phenomenon reflected the changes in the proteins involved in information processing such as replication, translation, and transcription. In addition, the 60 kDa heat-shock protein and protein-L-isoaspartate (D-aspartate) O-methyltransferase (*pcm2*), which are classified in a cellular processing and signaling group involved in maintaining protein structure and integrity, were also affected. These data indicate global changes in the metabolic pathways in the $\Delta omp43$ mutant.

RNA expression analysis of the identified proteins by RT-PCR

To verify the proteomics data, semi-quantitative RT-PCR analysis was performed to correlate gene expression with

protein expression. Fourteen of the 27 genes (*tldD* was duplicated) whose encoded proteins were found in the 2-DE analysis were selected for further investigation (Table 2). Although the mRNA expression of 6 genes was unchanged, that of the other 8 genes showed significant changes (Fig. 4). In RT-PCR analysis, the mRNA expressions of 6 targeted genes (*tldD*, *efp*, *nrX*, *pdhA*, *purB*, and ATPA) were lower, while those of 2 targeted genes (*Rho* and *yfeA*) were higher in $\Delta omp43$ than in the WT (panel A in Fig. 4). The density of each band was quantified by using scanning densitometry, and the expression was subsequently normalized to 16S mRNA expression (panel B in Fig. 4). The results were consistent with those obtained from the proteins identified in the MALDI-TOF-MS assay.

Discussion

The loss or decrease in OMP expression in several Gram-negative bacteria occasionally results in decreased proliferation and fitness *in vitro* and *in vivo*. For example, in *Haemophilus* species, *ompA*, which maintains cell structure and functions as a porin regulating the entry of nutrients into the bacterium, has been well established [37]. Additionally, OMP- or porin-deficient mutant strains have shown reduced growth or loss of viability in *Mycobacterium* species [24], *Salmonella enterica* [5], *Haemophilus ducreyi* [10], and *E. coli* [9].

However, the roles of OMPs in *B. henselae* have not yet been elucidated. Studies on OMPs in *B. henselae* have mainly focused on their primary role in host-bacterial interactions, and OMP43 has been suggested as the major adhesion protein in the outer membrane [6,7]. Burgess *et al.* [7] produced recombinant *E. coli* expressing the *B. henselae* OMP43 as a fusion protein for use in identifying the features of OMP43. Although they successfully determined the amino sequences and characterized the membrane topology of OMP43, as well as the attachment of OMP43 to HUVECs, the function of *omp43* has not yet been described [7]. Therefore, in this study, we established a $\Delta omp43$ mutant in *B. henselae*. In order to confirm that proliferation in $\Delta omp43$ was significantly lower than that of the WT, protein expression in $\Delta omp43$ was investigated by undertaking proteomic analysis and semi-quantitative RT-PCR.

Among the 20 protein spots that showed decreased expression in 2-DE, the mRNA expressions of the ATPA, *efp*, *nrX*, *pdhA*, *purB*, and *tldD* genes decreased in $\Delta omp43$. These proteins were mainly categorized based on their role in metabolism, based on their COG assignment (Table 3). This result suggested that the loss of OMP43 expression in $\Delta omp43$ disrupted energy metabolism, which might have affected cell growth.

Elongation factor P (*efp*) is a translation factor that can stimulate ribosomal peptidyl transferase activity and is homologous to the eukaryotic translation factors eIF5A and aIF5A [17]. Although eIF5A may not be absolutely essential for general protein synthesis, several studies have shown that *efp* is

Table 3. Decreased protein expression levels in *Bartonella henselae* $\Delta omp43$ compared with *B. henselae* wild-type strain (Houston-1) by MALDI-TOF-MS

Spot No.	Mascot score	Coverage (%)	Locus (primary annotation)	Protein identification by MALDI-TOF-MS (gene)	COG assignment	Predicted mass	Masses matched	Wild-type/ $\Delta omp43$	p/
386	151	39	gi 49476233	Succinate dehydrogenase flavoprotein subunit (<i>sdhA</i>)	Metabolism -energy production and conversion	67,387	23	2.0	6.04
467	128	46	gi 3603159	60 kDa heat-shock protein	Cellular processes and signaling -posttranslational modification, protein turnover, chaperones	53,127	20	*	4.90
483	183	51	gi 49476189	ATP synthase F0F1 subunit alpha (ATPA)	Metabolism -energy production and conversion	55,648	24	2.4	5.91
485	176	54	gi 49475378	Nitrogen regulation protein (<i>nrX</i>)	Function unknown	50,597	24	2.9	5.62
485	101	39	gi 49476189	ATP synthase F0F1 subunit alpha (ATPA)	Metabolism -energy production and conversion	55,648	16	2.9	5.91
498	100	49	gi 49476301	Dihydrolipoamide dehydrogenase (<i>phdD2</i>)	Metabolism -energy production and conversion	49,616	14	2.2	6.05
570	165	56	gi 49475235	Putative modulator of DNA gyrase (<i>tldD</i>)	Information storage and processing -replication, recombination and repair	50,933	22	2.7	6.33
570	153	54	gi 49475719	Adenylosuccinate lyase (<i>purB</i>)	Metabolism -nucleotide transport and metabolism	49,445	23	2.7	6.4
655	84	49	gi 49475961	Outer membrane protein 43	Cellular processes and signaling -cell wall/membrane/envelope biogenesis	44,311	12	*	8.52
659	84	43	gi 49475961	Outer membrane protein 43	Cellular processes and signaling -cell wall/membrane/envelope biogenesis	44,311	12	4.1	8.52
659	146	63	gi 49476065	Hypothetical protein BH14010	Not present in COG	41,120	18	4.1	6.99
665	212	47	gi 49475961	Outer membrane protein 43	Cellular processes and signaling -cell wall/membrane/envelope biogenesis	44,311	15	2.4	8.52
665	117	69	gi 49476065	Hypothetical protein BH14010	Not present in COG	41,120	23	2.4	6.99
748	119	44	gi 49475368	Pyruvate dehydrogenase E1 component subunit alpha (<i>pdhA</i>)	Metabolism -energy production and conversion	38,066	22	2.4	6.04
760	84	32	gi 49475823	Ketol-acid reductoisomerase	Metabolism -amino acid and coenzyme transport, and metabolism	37,725	14	2.2	6.08
871	67	39	gi 49475067	Hemin binding protein A (<i>hbpA</i>)	Metabolism -inorganic ion transport and metabolism	29,898	11	2.9	5.37
871	65	26	gi 3603169	60 kDa heat-shock protein	Cellular processes and signaling -posttranslational modification, protein turnover, chaperones	50,709	12	2.9	4.88
935	69	39	gi 49475425	ABC transporter periplasmic amino acid-binding protein	General function prediction only	28,390	8	2.7	5.54
1035	93	48	gi 49475323	50S ribosomal protein L9	Information storage and processing -translation, ribosomal structure and biogenesis	22,900	15	3.0	5.17

Table 3. Continued

Spot No.	Mascot score	Coverage (%)	Locus (primary annotation)	Protein identification by MALDI-TOF-MS (gene)	COG assignment	Predicted mass	Masses matched	Wild-type/ $\Delta omp43$	pI
1041	109	67	gi 49475323	50S ribosomal protein L9	Information storage and processing-translation, ribosomal structure and biogenesis	22,900	14	2.2	5.17
1041	99	58	gi 49476159	Elongation factor P (<i>efp</i>)	Information storage and processing-translation, ribosomal structure and biogenesis	21,456	11	2.2	5.21
1173	70	40	gi 49475636	Hypothetical protein BH08730	Not present in COG	22,659	12	2.2	8.99
1212	96	50	gi 49474947	3-Hydroxydecanoyl-(acyl-carrier-p rotein) dehydratase (<i>fabA</i>)	Metabolism-lipid transport and metabolism	19,017	17	2.2	5.28
1254	84	84	gi 49476168	Hypothetical protein BH15110	Not present in COG	14,749	12	2.2	5.75
1283	76	52	gi 49475926	Hypothetical protein BH12070	Not present in COG	21,747	10	*	9.41
1373	86	74	gi 49475397	50S ribosomal protein L7/L12	Information storage and processing-translation, ribosomal structure and biogenesis	12,707	9	6.8	4.81

Words in bold represent the name of four functional categories. MALDI-TOF-MS, matrix-assisted laser desorption ionization-time of flight-mass spectrometry; COG, Clusters of Orthologous Groups; pI, isoelectric point; ATP, adenosine triphosphate; ABC, ATP-binding cassette. *Not expressed proteins in mutant strain.

associated with viability, permeability, and fitness of bacteria [11,21,36,38]. The results showing downregulation of *efp* mRNA and protein expressions and the resulting lower growth rate of $\Delta omp43$ are consistent with previous data and reports. These results indicate that *omp43* might have a role in the integrity of the outer membrane in bacteria through downregulation of *efp* mRNA levels.

Two-component systems consist of sensor (*ntxY*) and regulator (*ntxX*) parts, which are reported to regulate metabolic and respiratory processes [29]. In *Azospirillum brasilense*, the *ntxXY* system might be involved in the regulation of nitrate assimilation [19]. The *ntxY* mutant of *Brucella abortus* showed lower survival within macrophages, which suggests that the *ntxXY* system is important for the intracellular viability of bacteria [8]. Attack *et al.* [3] used phylogenetic analysis to show that the *ntxX* response regulator is found in five distinct clades of pathogens: *Neisseria*, *Bartonella*, *Brucella*, *Ehrlichia*, and *Anaplasma*. It is possible that the *ntxXY* system is involved in the adaptation and survival of a variety of intracellular pathogens.

The pyruvate dehydrogenase complex (PDHC) converts pyruvate to acetyl-CoA through the serial reactions of three enzymes (E1, E2, and E3). The *phdA* gene encoding E1 enzymes in various bacteria has been studied and characterized [27]. Moreover, Schreiner *et al.* [33] showed that inactivation of the *aceE* (*aceE* is similar to *phdA*) gene resulted in an inability to grow in the presence of glucose and the loss of PDHC and E1 activities in *Corynebacterium glutamicum*. These results, along with the results of our current study, suggest that *phdA* may influence bacterial growth by altering metabolic pathways.

Adenylosuccinate lyase (*purB*) catalyzes the conversion of succinylaminoimidazole carboxamide ribotide to aminoimidazole carboxamide ribotide and fumarate or the conversion of adenylosuccinate to adenosine monophosphate and fumarate in the purine-biosynthetic pathway [25]. This indicates that purine nucleotides are essential for cell division. In humans, adenylosuccinate lyase deficiency causes growth retardation and is associated with central nervous system disorders [35]. The structural or chemical features of *purB* have been studied in bacteria such as *Bacillus subtilis*, *Staphylococcus aureus*, and *Thermotoga maritima* [16]. Although the function of *purB* in prokaryotes has not been established, our results suggest that *purB* might be involved in bacterial growth.

The F_0F_1 -ATP synthases, which catalyze the formation of adenosine triphosphate (ATP) from adenosine diphosphate and phosphate in most prokaryotes and eukaryotes, are membrane-bound enzymes that use the energy derived from a transmembrane electrochemical proton gradient. F_0F_1 -ATP synthases consist of two parts, F_0 and F_1 , which contain the subunits $\alpha_3\beta_3\gamma\delta\epsilon$ and ab_2c_{10-12} in *E. coli*. Functionally, the $\alpha_3\beta_3\delta ab_2$ subunits act as stators, while the $\gamma\epsilon c_{10-12}$ subunits are rotors [14]. These data suggest that ATPase, which is an

Table 4. Increased protein expression levels in *Bartonella henselae* $\Delta omp43$ compared with *B. henselae* wild-type strain (Houston-1) by MALDI-TOF-MS

Spot No.	Mascot score	Coverage (%)	Locus (primary annotation)	Protein description (gene)	COG assignment	Predicted mass	Masses matched	$\Delta omp43$ / wild-type	p/
327	264	65	gi 49475797	Elongation factor G (<i>fusA</i>)	Information storage and processing -translation, ribosomal structure and biogenesis	76,456	33	2.1	5.12
556	81	36	gi 49475235	Putative modulator of DNA gyrase (<i>tlfD</i>)	Information storage and processing -replication, recombination and repair	50,993	13	2.0	6.33
575	255	66	gi 49476319	Transcription termination factor <i>Rho</i>	Information storage and processing -transcription	47,429	33	2.1	5.47
755	130	49	gi 49476165	Glyceraldehyde-3-phosphate dehydrogenase (<i>gap</i>)	Metabolism -carbohydrate transport and metabolism	36,554	17	2.0	6.04
781	62	36	gi 49475018	L-asparaginase	Metabolism -amino acid transport and metabolism	36,042	9	2.2	5.83
886	133	52	gi 49475276	Hemin binding protein D (<i>hbpD</i>)	Metabolism -inorganic ion transport and metabolism	30,251	20	2.1	9.06
915	123	51	gi 49474908	Iron transport protein <i>yfeA</i>	Metabolism -inorganic ion transport and metabolism	33,766	15	2.1	6.01
995	97	49	gi 49475809	Protein-L-isoaspartate(D-aspartate) O-methyltransferase (<i>pcm2</i>)	Cellular processes and signaling -posttranslational modification, protein turnover, chaperones	24,570	13	2.5	5.14

Words in bold represent the name of four functional categories. MALDI-TOF-MS, matrix-assisted laser desorption ionization-time of flight-mass spectrometry; COG, Clusters of Orthologous Groups; p/, isoelectric point.

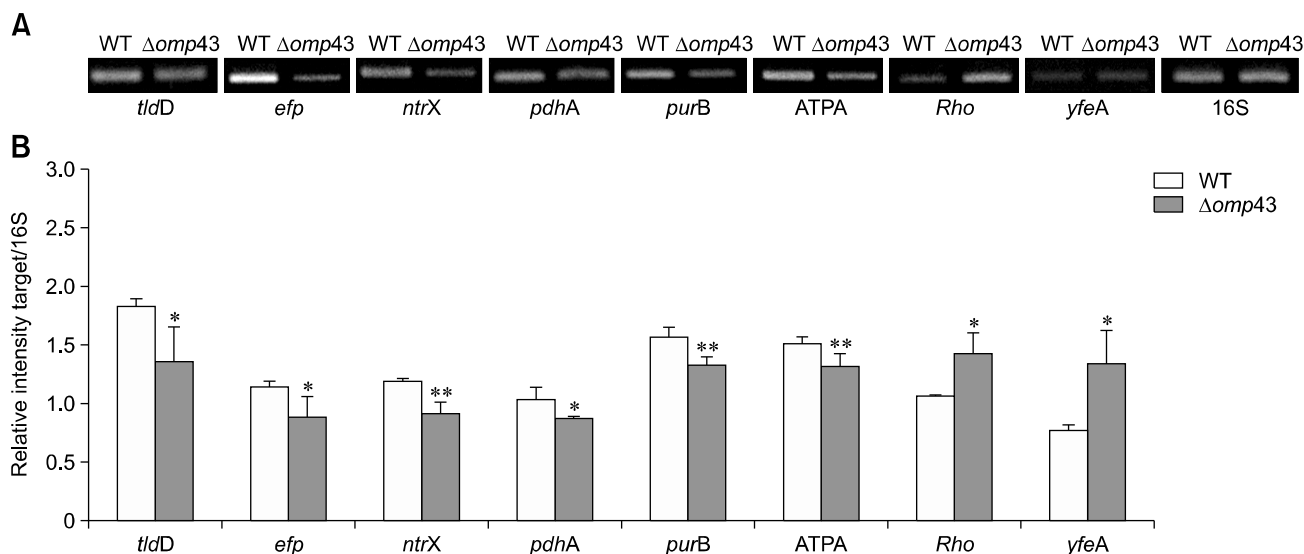


Fig. 4. Reverse transcriptase polymerase chain reaction (RT-PCR) analysis of target gene mRNAs (*tldD*, *efp*, *ntrX*, *pdhA*, *purB*, *ATPA*, *Rho*, and *yfeA*) between the wild-type (WT) and mutant ($\Delta omp43$) strains. (A) Agarose gel electrophoresis showing representative RT-PCR results. (B) Relative intensities of the PCR bands were quantified by scanning densitometry. Each datum represents the mean \pm SD (error bars) obtained from triplicate cultures of a representative experiment out of three performed. Data are expressed as ratios of target mRNA normalized to 16S mRNA. Data significance was evaluated with a Student's *t*-test; **p* < 0.05, ***p* < 0.01.

F₀F₁-ATP synthase, might affect ATP synthesis.

The *tldD* gene is associated with the activity of DNA gyrase in *E. coli*. Additionally, the protein products of the *tldD* and *tldE* genes regulate the stability of the *ccdA* and *ccdA41* antidotes and are essential for MccB17 maturation in *E. coli* [1]. These results suggest that *tldD* gene products are involved in protein processing and degradation.

Decreased expression of the above-mentioned genes in $\Delta omp43$ might be affected by the loss of OMP43 expression. Therefore, the retarded growth in $\Delta omp43$ was possibly induced by metabolic pathways altered as a result of the decrease in the expressions of these genes. In contrast, eight protein spots showed increased expression in the 2-DE analysis, and among those, the mRNA expression levels of *Rho* and *yfeA* were increased in $\Delta omp43$. Additionally, based on COG assignment, *Rho* and *yfeA* are categorized as being important in transcription and metabolism, respectively (Table 4). The increased expression of these genes might contribute to functional compensation for the absence of OMP43 expression in $\Delta omp43$.

The colonization and growth of many bacterial pathogens is affected by their ability to invade mammalian hosts to obtain iron. However, the iron in host cells is strongly bound by ferritin, transferrin, and lactoferrin [18]. The ATP-binding cassette (ABC) transport system is a well-characterized uptake system. In *Yersinia pestis*, the *yfe* locus is composed of five genes (*yfeA-E*) and forms a system similar to the ABC transport system associated with the acquisition of inorganic iron and other ions. Moreover, it has been reported that *yfe* affects the growth of *Y. pestis* [4]. Although a detailed study on the ABC

transport system of *B. henselae* has not been undertaken, it has been reported that the acquisition of heme compounds such as hemin, erythrocyte membrane fractions, and hemoglobin is essential for the growth and survival of the bacterium [32]. Hence, an upregulated *yfeA* expression in $\Delta omp43$ might be a mechanism to compensate for energy loss due to alterations in the metabolic pathways.

The bacterial transcriptional terminators have two types of pathways: factor-independent (intrinsic) and factor-dependent (*Rho*-dependent) [30]. The *Rho*-dependent pathway serves to terminate the synthesis of transcripts. Recently, Leela *et al.* [23] reported that *Rho*-dependent transcription termination is necessary to avoid the excessive genome-wide R-loops in *E. coli*. The observation that *Rho* expression was increased in $\Delta omp43$ suggests that *Rho*-dependent transcription termination is associated with repair of disrupted transcription occurring because of gene manipulation or other changes. However, further studies are needed to confirm this hypothesis.

In conclusion, the $\Delta omp43$ strain, which is the first *omp43*-deficient bacterial strain generated by using electrophoresis, showed significantly decreased proliferation. The changes in the mRNA expressions of genes in $\Delta omp43$ were mainly associated with metabolic processes. Although the possibility that other undetected proteins or genes may display altered expression or function to compensate for the loss of OMP43 cannot be ruled out, our data suggest that the growth retardation in $\Delta omp43$ is induced by altered metabolic pathways and will provide useful information for further investigation of the mechanisms underlying this effect.

Acknowledgments

This research was supported by Basic Science Research Program through the National Research Foundation of Korea (NRF) funded by the Ministry of Education, Science and Technology (2010-0012319).

Conflict of Interest

The authors declare no conflicts of interest.

References

- Allali N, Afif H, Couturier M, Van Melderen L. The highly conserved TldD and TldE proteins of *Escherichia coli* are involved in microcin B17 processing and in CcdA degradation. *J Bacteriol* 2002, **184**, 3224-3231.
- Anderson BE, Neuman MA. *Bartonella* spp. as emerging human pathogens. *Clin Microbiol Rev* 1997, **10**, 203-219.
- Atack JM, Srikhanta YN, Djoko KY, Welch JP, Hasri NH, Steichen CT, Vanden Hoven RN, Grimmond SM, Othman DS, Kappler U, Apicella MA, Jennings MP, Edwards JL, McEwan AG. Characterization of an *ntrX* mutant of *Neisseria gonorrhoeae* reveals a response regulator that controls expression of respiratory enzymes in oxidase-positive proteobacteria. *J Bacteriol* 2013, **195**, 2632-2641.
- Bearden SW, Perry RD. The Yfe system of *Yersinia pestis* transports iron and manganese and is required for full virulence of plague. *Mol Microbiol* 1999, **32**, 403-414.
- Bucarey SA, Villagra NA, Martinic MP, Trombert AN, Santiviago CA, Maulén NP, Youderian P, Mora GC. The *Salmonella enterica* serovar Typhi *tsx* gene, encoding a nucleoside-specific porin, is essential for prototrophic growth in the absence of nucleosides. *Infect Immun* 2005, **73**, 6210-6219.
- Burgess AW, Anderson BE. Outer membrane proteins of *Bartonella henselae* and their interaction with human endothelial cells. *Microb Pathog* 1998, **25**, 157-164.
- Burgess AW, Paquet JY, Letesson JJ, Anderson BE. Isolation, sequencing and expression of *Bartonella henselae omp43* and predicted membrane topology of the deduced protein. *Microb Pathog* 2000, **29**, 73-80.
- Carrica Mdel C, Fernandez I, Martí MA, Paris G, Goldbaum FA. The NtrY/X two-component system of *Brucella* spp. acts as a redox sensor and regulates the expression of nitrogen respiration enzymes. *Mol Microbiol* 2012, **85**, 39-50.
- Darcan C, Ozkanca R, Flint KP. Survival of nonspecific porin-deficient mutants of *Escherichia coli* in black sea water. *Lett Appl Microbiol* 2003, **37**, 380-385.
- Davie JJ, Campagnari AA. Comparative proteomic analysis of the *Haemophilus ducreyi* porin-deficient mutant 35000HP::P2AB. *J Bacteriol* 2009, **191**, 2144-2152.
- de Crécy E, Metzgar D, Allen C, Pénicaud M, Lyons B, Hansen CJ, de Crécy-Lagard V. Development of a novel continuous culture device for experimental evolution of bacterial populations. *Appl Microbiol Biotechnol* 2007, **77**, 489-496.
- de Maagd RA, Mulders IH, Canter Cremers HC, Lugtenberg BJ. Cloning, nucleotide sequencing, and expression in *Escherichia coli* of a *Rhizobium leguminosarum* gene encoding a symbiotically repressed outer membrane protein. *J Bacteriol* 1992, **174**, 214-221.
- Dehio C, Meyer M, Berger J, Schwarz H, Lanz C. Interaction of *Bartonella henselae* with endothelial cells results in bacterial aggregation on the cell surface and the subsequent engulfment and internalisation of the bacterial aggregate by a unique structure, the invasome. *J Cell Sci* 1997, **110**, 2141-2154.
- Diez M, Zimmermann B, Börsch M, König M, Schweinberger E, Steigmiller S, Reuter R, Felekyan S, Kudryavtsev V, Seidel CA, Gräber P. Proton-powered subunit rotation in single membrane-bound F₀F₁-ATP synthase. *Nat Struct Mol Biol* 2004, **11**, 135-141.
- Fuhrmann O, Arvand M, Göhler A, Schmid M, Krüll M, Hippenstiel S, Seybold J, Dehio C, Suttrop N. *Bartonella henselae* induces NF-kappaB-dependent upregulation of adhesion molecules in cultured human endothelial cells: possible role of outer membrane proteins as pathogenic factors. *Infect Immun* 2001, **69**, 5088-5097.
- Fyfe PK, Dawson A, Hutchison MT, Cameron S, Hunter WN. Structure of *Staphylococcus aureus* adenylosuccinate lyase (PurB) and assessment of its potential as a target for structure-based inhibitor discovery. *Acta Crystallogr D Biol Crystallogr* 2010, **66**, 881-888.
- Ganoza MC, Kiel MC, Aoki H. Evolutionary conservation of reactions in translation. *Microbiol Mol Biol Rev* 2002, **66**, 460-485.
- Gray-Owen SD, Schryvers AB. Bacterial transferrin and lactoferrin receptors. *Trends Microbiol* 1996, **4**, 185-191.
- Ishida ML, Assumpção MC, Machado HB, Benelli EM, Souza EM, Pedrosa FO. Identification and characterization of the two-component NtrY/NtrX regulatory system in *Azospirillum brasilense*. *Braz J Med Biol Res* 2002, **35**, 651-661.
- Kaiser PO, Riess T, Wagner CL, Linke D, Lupas AN, Schwarz H, Raddatz G, Schäfer A, Kempf VA. The head of *Bartonella* adhesin A is crucial for host cell interaction of *Bartonella henselae*. *Cell Microbiol* 2008, **10**, 2223-2234.
- Kang HA, Hershey JW. Effect of initiation factor eIF-5A depletion on protein synthesis and proliferation of *Saccharomyces cerevisiae*. *J Biol Chem* 1994, **269**, 3934-3940.
- Koehler JE, Sanchez MA, Garrido CS, Whitfeld MJ, Chen FM, Berger TG, Rodríguez-Barradas MC, LeBoit PE, Tappero JW. Molecular epidemiology of *Bartonella* infections in patients with bacillary angiomatosis-peliosis. *N Engl J Med* 1997, **337**, 1876-1883.
- Leela JK, Syeda AH, Anupama K, Gowrishankar J. Rho-dependent transcription termination is essential to prevent excessive genome-wide R-loops in *Escherichia coli*. *Proc Natl Acad Sci U S A* 2013, **110**, 258-263.
- Mailaender C, Reiling N, Engelhardt H, Bossmann S, Ehlers S, Niederweis M. The MspA porin promotes growth and increases antibiotic susceptibility of both *Mycobacterium bovis* BCG and *Mycobacterium tuberculosis*. *Microbiology*

- 2004, **150**, 853-864.
25. **Mueller EJ, Meyer E, Rudolph J, Davisson VJ, Stubbe J.** *N*⁵-carboxyaminoimidazole ribonucleotide: evidence for a new intermediate and two new enzymatic activities in the *de novo* purine biosynthetic pathway of *Escherichia coli*. *Biochemistry* 1994, **33**, 2269-2278.
 26. **Nakae T.** Outer membrane of *Salmonella*. Isolation of protein complex that produces transmembrane channels. *J Biol Chem* 1976, **251**, 2176-2178.
 27. **Neveling U, Bringer-Meyer S, Sahm H.** Gene and subunit organization of bacterial pyruvate dehydrogenase complexes. *Biochim Biophys Acta* 1998, **1385**, 367-372.
 28. **Nikaido H, Vaara M.** Molecular basis of bacterial outer membrane permeability. *Microbiol Rev* 1985, **49**, 1-32.
 29. **Pawlowski K, Klose U, de Bruijn FJ.** Characterization of a novel *Azorhizobium caulinodans* ORS571 two-component regulatory system, NtrY/NtrX, involved in nitrogen fixation and metabolism. *Mol Gen Genet* 1991, **231**, 124-138.
 30. **Peters JM, Vangeloff AD, Landick R.** Bacterial transcription terminators: the RNA 3'-end chronicles. *J Mol Biol* 2011, **412**, 793-813.
 31. **Regnery RL, Anderson BE, Clarridge JE 3rd, Rodriguez-Barradas MC, Jones DC, Carr JH.** Characterization of a novel *Rochalimaea* species, *R. henselae* sp. nov., isolated from blood of a febrile, human immunodeficiency virus-positive patient. *J Clin Microbiol* 1992, **30**, 265-274.
 32. **Sander A, Kretzer S, Brecht W, Oberle K, Bereswill S.** Hemin-dependent growth and hemin binding of *Bartonella henselae*. *FEMS Microbiol Lett* 2000, **189**, 55-59.
 33. **Schreiner ME, Fiur D, Holátko J, Pátek M, Eikmanns BJ.** E1 enzyme of the pyruvate dehydrogenase complex in *Corynebacterium glutamicum*: molecular analysis of the gene and phylogenetic aspects. *J Bacteriol* 2005, **187**, 6005-6018.
 34. **Seki N, Sasaki T, Sawabe K, Sasaki T, Matsuoka M, Arakawa Y, Marui E, Kobayashi M.** Epidemiological studies on *Bartonella quintana* infections among homeless people in Tokyo, Japan. *Jpn J Infect Dis* 2006, **59**, 31-35.
 35. **Spiegel EK, Colman RF, Patterson D.** Adenylosuccinate lyase deficiency. *Mol Genet Metab* 2006, **89**, 19-31.
 36. **Woese CR, Stackebrandt E, Weisburg WG, Paster BJ, Madigan MT, Fowler VJ, Hahn CM, Blanz P, Gupta R, Neelson KH, Fox GE.** The phylogeny of purple bacteria: the alpha subdivision. *Syst Appl Microbiol* 1984, **5**, 315-326.
 37. **Zhang B, Xu C, Zhou S, Feng S, Zhang L, He Y, Liao M.** Comparative proteomic analysis of a *Haemophilus parasuis* SC096 mutant deficient in the outer membrane protein P5. *Microb Pathog* 2012, **52**, 117-124.
 38. **Zou SB, Hersch SJ, Roy H, Wiggers JB, Leung AS, Buranyi S, Xie JL, Dare K, Ibba M, Navarre WW.** Loss of elongation factor P disrupts bacterial outer membrane integrity. *J Bacteriol* 2012, **194**, 413-425.